Published in final edited form as:

New Phytol. 2016 April ; 210(2): 525–534. doi:10.1111/nph.13790.

Cytochrome P450 promiscuity leads to a bifurcating biosynthetic pathway for tanshinones

Juan Guo[1,*], **Xiaohui Ma**[1,6,*], **Yuan Cai**[1,2], **Ying Ma**[1], **Zhilai Zhan**[1], **Yongjin J Zhou**[2], **Wujun Liu**[2], **Mengxin Guan**[3], **Jian Yang**[1], **Guanghong Cui**[1], **Liping Kang**[1], **Lei Yang**[4], **Ye Shen**[1], **Jinfu Tang**[1], **Huixin Lin**[1], **Xiaojing Ma**[1], **Baolong Jin**[1], **Zhenming Liu**[3], **Reuben J. Peters**[5], **Zongbao K. Zhao**[2,#], and **Luqi Huang**[1,#]

[1]State Key Laboratory Breeding Base of Dao-di Herbs, National Resource Center for Chinese Materia Medica, China Academy of Chinese Medical Sciences, Beijing, 100700, P. R. China

[2]Division of Biotechnology, Dalian Institute of Chemical Physics, CAS, Dalian, 116023, P.R. China

[3]State Key Laboratory of Natural and Biomimetic Drugs, School of Pharmaceutical Sciences, Peking University, Beijing 100191, P. R. China

[4]Plant Science Research Center, Shanghai Chenshan Botanical Garden, Shanghai Key Laboratory of Plant Functional Genomics and Resources, Shanghai 201602, P.R. China

[5]Roy J. Carver Department of Biochemistry, Biophysics, and Molecular Biology, Iowa State University, Ames, IA 50011, USA

[#]**Corresponding authors:** Luqi Huang, Tel: 86-10-84044340. huangluqi01@126.com, Zongbao K. Zhao, Tel: 86-411-84379211. zhaozb@dicp.ac.cn.

[*]These authors contributed equally to this work.

Author Contribution

J.G., X.M., Y.C., Z.K.Z. and L.H. planned and designed research. J.G., X.M., Y.C., Y.M., Z.Z., Y.J.Z., W.L., and X.M. performed experiments. J.G., X.M., Y.C., Y.M., Z.Z., Y.J.Z., W.L., M.G., Y.J., G.C., L.K., L.Y., Y.S., J.T., H.L., X.M., R.J.P. and B.J. analyzed data. J.G., X.M. Y.M., Z.Z., Y.J.Z., M.G., Z.L., R.J.P., Z.K.Z., and L.H. wrote the paper.

Supporting Information

Additional supporting information may be found in the online version of this article.

Fig. S1 Coexpression analysis of up-regulated CYPs with *CYP76AH1*.

Fig. S2 Characterization of 11-hydroxy ferruginol (**6**).

Fig. S3 LC-MS analysis of *in vitro* enzymatic assay of CYP76AH3 using 11-hydroxy ferruginol (**6**) as substrate to produce 11-hydroxy sugiol (**8**), or CYP76AK1, using 11-hydroxy ferruginol (**6**) as substrate to produce 11,20-dihydroxy ferruginol (**9**), and 10-hydroxymethyl tetrahydromiltirone (**10**) compared with control.

Fig. S4 LC-MS analysis of *in vitro* enzymatic assay of CYP76AH3 using sugiol (**7**) as substrate to produce 11-hydroxy sugiol (**8**) compared with control.

Fig. S5 Characterization of 11,20-dihydroxy ferruginol (**9**).

Fig. S6 Characterization of 10-hydroxymethyl tetrahydromiltirone (**10**).

Fig. S7 LC-MS analysis of *in vitro* enzymatic assay of CYP76AK1 using 11-hydroxy sugiol (**8**) as substrate to produce 11,20-dihydroxy sugiol (**11**) compared with control.

Fig. S8 Characterization of 11,20-dihydroxy sugiol (**11**).

Fig. S9 Detection of oxygenated terpenoids intermediates in rhizome of Danshen.

Fig. S10 Relative expression of the known CYPs in *CYP76AH3*-RNAi and *CYP76AK1*-RNAi hairy root lines compared with control.

Fig. S11 Sequence alignment of CYP76AK1 with template (PDB code: 2HI4). Deep blue shows the conserved residues in template sequences.

Fig. S12 PROCHECK Ramachandran plot of CYP76AK1 model showing the distribution of residues in favored (red), allowed (yellow) and outlier regions (white). Squares and triangles represent normal amino acids and glycine residues respectively. Red labels show residues in less allowed regions.

Table S1 Primers used in this study.

Table S2 *S. cerevisiae* strains used in this study. This material is available free of charge via the Internet at http://pubs.acs.org.

[6]Pharmacy College, Chengdu University of Traditional Chinese Medicine, Chengdu, 611137, P.R. China

Summary

- Cytochromes P450 (CYPs) play key role in generating the structural diversity of terpenoids, the largest group of plant natural products. However, functional characterization of CYPs has been challenging because of the expansive families found in plant genomes, diverse reactivity and inaccessibility of their substrates and products.
- Here we present the characterization of two CYPs, CYP76AH3 and CYP76AK1, that act sequentially to form a bifurcating pathway for the biosynthesis of tanshinones, the oxygenated diterpenoids from the Chinese medicinal plant Danshen.
- These CYPs had similar transcription profiles to that of the known gene responsible for tanshinone production in elicited Danshen hairy roots. Biochemical and RNA interference studies demonstrated that both CYPs are promiscuous. CYP76AH3 oxidizes ferruginol at two different carbon centers, and CYP76AK1 hydroxylates C-20 of two of the resulting intermediates. Together, these convert ferruginol into 11,20-dihydroxy ferruginol and 11,20-dihydroxy sugiol en route to tanshinones. Moreover, we demonstrate the utility of these CYPs by engineering yeast for heterologous production of six oxygenated diterpenoids, which in turn enabled structural characterization of three novel compounds produced by CYP-mediated oxidation.
- Our results highlight the incorporation of multiple CYPs in diterpenoids metabolic engineering, and a continuing trend of CYPs promiscuity generating complex networks in terpenoid biosynthesis.

Keywords

Cytochrome P450 monooxygenases; diterpenoids biosynthesis; enzymatic promiscuity; metabolic pathways; *Salvia miltiorrhiza* Bunge; synthetic biology

Introduction

Terpenoids represent the largest group of plant natural products, with over 54,000 structurally defined compounds. Many terpenoids have diverse biological activities and, thus, have been widely used as pharmaceuticals and medicines (Gershenzon & Dudareva, 2007). For example, artemisinin and taxol are widely used agents in the treatment of malaria and cancer, respectively. Cytochrome P450 (CYP) enzymes are major players in generating the structural diversity of terpenoids, as more than 97% of the terpenoids are oxygenated via the biological activity of CYPs (Ashour *et al.*, 2010; Hamberger & Bak, 2013; Renault *et al.*, 2014). In fact, CYPs represent the biggest superfamily of enzymes (approximately 1% of all protein encoding genes) in plants (Renault *et al.*, 2014). While hydroxylation is the most commonly catalyzed reaction, CYPs can also catalyze many mechanistically more complex reactions (Mizutani & Sato, 2011). In addition to the typical regio- and stereo-specific

hydroxylation reactions (Renault *et al.*, 2014), there are increasingly more examples of CYPs exhibiting promiscuity by accepting multiple substrates and/or producing multiple products (Ro *et al.*, 2005; Swaminathan *et al.*, 2009; Seki *et al.*, 2011; Wang *et al.*, 2012; Wu *et al.*, 2013). The abundance of CYPs in plant genomes, together with their promiscuity, is one of the primary drivers of the chemical diversity of terpenoids. However, this presents daunting challenges to the identification of CYPs associated with the biosynthesis of particular natural products. For example, in the model plant *Arabidopsis thaliana*, more than 70% of CYPs remain functionally uncharacterized (Bak *et al.*, 2011). Therefore, functional characterization of plant CYPs is of general interest towards increasing our understanding of plant metabolism, and can provide valuable elements for metabolic engineering (Bak *et al.*, 2011).

Tanshinones are a group of abietane *nor*-diterpenoid quinone natural products found in the Chinese medicinal plant *Salvia miltiorrhiza* Bunge (also known as Danshen), which have been widely used in clinical for the treatment of cerebrovascular- and cardiovascular-related diseases (Zhou *et al.*, 2005; Dong *et al.*, 2011). The Fufang Danshen Dripping Pill, with Danshen as one of the major components, is widely used in China. The Pill also has been approved for phase III clinical trials in USA (Clinical Trials.gov Identifier: NCT01659580). There have been more than 40 tanshinones and structurally related compounds identified from Danshen. Studies have demonstrated that various tanshinones, such as tanshinone IIA (**1**), cryptotanshinone (**2**) and tanshinone I (**3**) (Fig. 1a), have antibacterial, antioxidant, anti-inflammation, and anti-cancer activities (Zhou *et al.*, 2005; Dong *et al.*, 2011; Robertson *et al.*, 2014). While tanshinones can be extracted from Danshen roots, the ever-growing demand cannot be met by cultivation of Danshen plants. Thus, attempts have been made to improve tanshinones production in Danshen hairy root cultures by enhancing the expression of key enzymes involved in the general isoprenoid/terpenoids precursor biosynthetic pathway (Kai *et al.*, 2011). In addition, a synthetic biology approach has been employed to engineer the production of potential intermediates of tanshinone biosynthesis in recombinant *Saccharomyces cerevisiae* (yeast) (Dai *et al.*, 2012; Zhou *et al.*, 2012; Guo *et al.*, 2013). However, the tanshinone biosynthetic pathway remains incompletely elucidated, particularly the latter modification steps, which impedes the application of such rational approaches to improve access to the tanshinones.

The formation of tanshinones is initiated by cyclization of (*E,E,E*)-geranylgeranyl diphosphate (GGPP), the general diterpenoid precursor, to the abietane miltiradiene (**4**), which is mediated by two enzymes, SmCPS1 and SmKSL1 (Fig. 1b) (Gao *et al.*, 2009; Cheng *et al.*, 2013). To transform **4** into tanshinones, multiple reactions are required, including oxidation, hetero-cyclization, aromatization and de-methylation, all of which fall into the repertoire of known CYP-mediated reactions (Mizutani & Sato, 2011). We previously demonstrated that **4** is the precursor to tanshinones, and identified a CYP, CYP76AH1, that can produce ferruginol (**5**) (Guo *et al.*, 2013; Zi & Peters, 2013). In this study, two CYPs (*CY76AH3* and *CYP76AK1*) were found to exhibit similar transcription profiles as *CYP76AH1* in elicited Danshen hairy roots. Further biochemical analysis and RNA-interference (RNAi) in Danshen hairy root cultures suggested that both CYPs are promiscuous and act sequentially to form a bifurcating pathway for tanshinone biosynthesis.

When utilized in engineered yeast, these genes led to the production of six oxygenated diterpenoids, which provide materials for further biological study and the identification of subsequently acting CYPs. Our results further emphasize the utility of such a synthetic biology approach to characterization of plant CYPs (Kitaoka *et al.*, 2015), and continued critical examination of the effect of CYP promiscuity on the complex nature of terpenoid biosynthesis (Wang *et al.*, 2012; Wu *et al.*, 2013).

Materials and Methods

Plant materials and chemicals

S. miltiorrhiza plants used to analyze organ specific CYP expression were collected in Beijing, China. Ferruginol and sugiol were purchased from BioBioPha (Yunnan, China). Tanshinone I, cryptotanshinone, tanshinone IIA and 11-hydroxy-sugiol were purchased from Chengdu Must Bio-Technology Co., Ltd (Sichuan, China). The purity of these commercial chemicals was >95% (HPLC).

Heterologous expression in yeast and *in vitro* enzymatic activity assay

Full-length cDNAs of *CYP76AH3* (Accession No. KR140168) and *CYP76AK1* (Accession No. KR140169) were cloned as previously described (Guo *et al.*, 2013), using the primers shown in Table S1. The open reading frame of *CYP76AH3* was sub-cloned into the yeast epitope-tagged vector pESC-His using *BamH*I and *Sal*I restriction sites, yielding pESC-His::*CYP76AH3*. The open reading frame of *CYP76AK1* was sub-cloned, using *EcoR*I and *Spe*I restriction sites, into plasmid pESC-His and pESC-His::*CYP76AH3*, yielding pESC-His::*CYP76AK1* and pESC-His::*CYP76AH3/CYP76AK1*. These plasmids were transformed into the yeast strain WAT11 that enables catalytic activity of plant CYPs by also expressing ATR1 (Urban *et al.*, 1997). Yeast cultures were grown and microsomes prepared as described previously (Pompon *et al.*, 1996; Guo *et al.*, 2013).

In vitro enzymatic activity assays were performed on a shaking incubator (150 rpm), at 30 °C for 4 hour in 500 μL of 100 mM Tris-HCl, pH 7.5, containing 0.5 mg total microsomal proteins, 500 μM NADPH, along with a regenerating system (consisting of 5 μM FAD, 5 μM FMN, 5 mM glucose-6-phosphate, 1 Unit/mL glucose-6-phosphate dehydrogenase), and 100 μM of either miltiradiene (**4**), ferruginol (**5**), sugiol (**6**), or 11-hydroxy sugiol (**8**). Reactions were stopped by addition of 500 μL of n-hexane and vortexing. Negative control reactions were carried out with microsomal preparations from recombinant yeast transformed with ‘empty’ pESC-His.

To produce sufficient amounts of the unknown CYP76AK1 product **11** for chemical structure characterization, these *in vitro* assays were scaled up. Microsomes were prepared from 4 L of yeast expressing *CYP76AK1*. These were used in a 40 mL reaction, with the buffer and NADPH regeneration system described above, and 20 mg of 11-hydroxy-sugiol (**8**) as substrate. The assay was performed on a shaking incubator (150 rpm), at 30 °C for 30 h. The incubation products were extracted and **11** purified, using the methods described below, for chemical structure analysis by NMR.

RNA interference in hairy root of Danshen

Gene specific fragments of *CYP76AH3* (nucleotides 636–1038) and *CYP76AK1* (nucleotides 651–1054) were cloned into the pENTR vector using the Directional TOPO Cloning Kits (Invitrogen) and the primers shown in Table S1, and further sub-cloned into the hpRNA binary vector pK7GWIWG2D using Gateway LR Clonase Enzyme Mix (Invitrogen) to generate RNAi knock-down vectors. Each of these constructs was introduced into *A. rhizogenes* C58C1 via a freeze-thaw transformation method (Weigel & Glazebrook, 2005). These recombinant *A. rhizogenes* were then transfected into Danshen leaf explants, using *A. rhizogenes* C58C1 harboring 'empty' pK7GWIWG2D(II) as a negative control, and the resulting transformed explants were used to generate hairy root cultures, as previously described (Cheng *et al.*, 2013; Cheng *et al.*, 2014). The transformed hairy root lines were cultured in 1/2 MS solid medium at 25 °C in the dark for 6–8 weeks and tissue then collected for qRT-PCR and metabolite analysis, as described below.

Quantitative real-time PCR analysis

Total RNA was extracted from *S. miltiorrhiza* or RNAi transformed hairy root cultures using TRIzol reagent (Invitrogen) following the manufactures' directions. First-strand cDNA was synthesized using the PrimeScriptR RT reagent Kit with gDNA Eraser (Takara, Tokyo, Japan). Relative transcript abundance was determined by qRT-PCR using the SYBR Premix Ex Taq II system (Takara, Tokyo, Japan) on an ABI 7500 instrument (Applied Biosystems, Foster City, CA, USA). The primers used for qRT-PCR analysis are listed in Table S1. The gene for actin was used as the endogenous control. At least three independent experiments were performed for each analysis.

Engineering yeast for production of oxygenated tanshinones intermediates

To engineer yeast for production of intermediates from tanshinone biosynthesis, and obtain enough compound for structural characterization, pESC-His::*CYP76AK1* or pESC-His::*CYP76AH3/CYP76AK1* were transformed into the ferruginol (**5**) production strain YJ35, using lithium acetate/single-stranded carrier DNA/polyethylene glycol transformation method (Daniel Gietz & Woods, 2002; Zhou *et al.*, 2012), to produce the YJ51 and the YJ61 strains (the genotype and characteristics of each of these are listed in Table S2). Transformants were selected on YNB medium containing 20 g/L glucose and grown at 30 °C for 48 h. The recombinant yeast strains were grown in YNB medium containing 2% glucose (YNB/glucose) at 30 °C, shaking at 250 rpm, for 48 h, then transferred to 50 mL YNB/glucose medium in 250-mL flasks and grown to an initial OD600 of 0.05, and cultivated an additional 12–16 h to reach logarithmic phase. Cells were centrifuged and washed twice with sterile water to remove any residual glucose. The cells were then resuspended in 50 mL YNB medium containing 2% galactose (YNB/gal) for induction, and grown for 30–72 h to produce diterpenoids.

In order to simplify the fermentation procedure, the inducible promoters in the pESC-His vector were replaced by constitutive promoters from yeast. The constitutive promoters TEF1p and PGK1p were amplified from the genomic DNA of *S. cerevisiae* strain BY4741, and used to replace the GAL10 and GAL1 promoters, respectively, in pESC-His by overlap extension PCR. This replacement resulted in the plasmid pESC-TP. *CYP76AH3* and

CYP76AK1 were sub-cloned downstream of the TEF1p and PGK1p promoter, respectively, using a previously described RF cloning strategy (Zhou *et al.*, 2011). The resulting pESC-TP::*CYP76AH3/CYP76AK1* construct was confirmed by PCR screening and sequencing, and then transformed into YJ35, resulting in YJ62 (the genotype and characteristics of which are listed in Table S2).

Strain YJ62 was used for production of oxygenated tanshinones intermediates through fed-batch fermentation. YJ62 was first inoculated into 1 L flask containing 0.2 L YNB medium, and grown at 30 °C. This starter culture was then transferred to a 5 L fermentor (GS-8000-P, ShanhaiGuangshi, Shanghai, China) containing 2 L YNB medium. Fermentation was carried out at 30 °C and 250 rpm. During fermentation, the dissolved oxygen was controlled at >40% saturation, and the pH was controlled and held at 4. Concentrated glucose solution (40%, wt/vol) was fed periodically to keep the glucose concentration above 1.0 g/L. Additional YNB (6.7g/L) was fed after the initial 30 h of fermentation. The culture was then harvested by extraction after 72 h total fermentation time.

Homology modeling and docking analysis

Template selection was carried out by BLAST search (Altschul *et al.*, 1997) of the CYP76AK1 amino acid sequence against the Protein Data Bank (PDB). The CYP76AK1 model was constructed using DISCOVERY STUDIO v2.5 (http://www.accelrys.com). The model with the highest score was validated by PROCHECK (Laskowski *et al.*, 1993).

Compounds **5**, **6**, **7**, **8** were docked into CYP76AK1 using AutoDock 4.0 (Morris *et al.*, 1998). A grid size of 40×40×40 Å with grid point spacing of 0.375Å was set for ligand docking. Each compound was subjected to 100 runs of the AutoDock search using the Lamarckian genetic algorithm; all other parameters were set to default values.

Metabolite extraction

In vitro enzymatic assays were extracted with an equal volume of n- hexane, which was separated and subjected to GC-MS and LC-MS analysis. Yeast cultures were extracted three times by ultrasonication with an equal volume of n-hexane. After separation, the organic extract was concentrated under vacuum, and the residue resuspended in n-hexane. For isolation of compound **6**, the residue was loaded on silica gel column and eluted with a 20:1 mixture of petroleum ether and ethyl acetate (V/V). Other diterpenoid products were purified by preparative HPLC, as described below. To determine the content of these compounds in hairy root cultures, approximately 25 mg of lyophilized tissue was extracted three times by ultrasonication in 1 mL methanol, the filtered extract then dried under vacuum, and resuspended in 120 μL acetonitrile for LC-MS analysis, as described below.

LC-MS, GC-MS and NMR analysis

GC-MS was carried out using a Trace 1310 series GC with detection via a TSQ8000 MS (Thermo Fisher Scientific Co. Ltd.). Chromatographic separation was performed on a TR-5ms column capillary column (30 m × 0.25 mm ID DF = 0.25 μm; Thermo Fisher Scientific Co. Ltd.). Helium was used as the carrier gas at a constant flow rate of 1 mL/min through the column. The injector temperature was set at 280 °C. The temperature gradient

program was: 50 °C (1 min), 50 → 150 °C at 5 °C/min, 150 → 230 °C at 20 °C/min, 230 → 300 °C linear at 30 °C/min, 300 °C (5 min). Each run analyzed 1 μL injections of the relevant sample using a 50:1 split ratio.

LC-MS was carried out using an Acquity UPLCTM system (Waters Corp., Milford, MA, USA) with an Acquity UPLC BEH C18 column (50 × 2.1 mm, 1.7 μm). The column temperature was set at 40 °C. The flow rate was kept at 500 μL/min. Mobile phases were water (A) and acetonitrile (B). The gradient was as follows: (0~8.0) min, 50%→80% B; (8.0~8.5) min, 80%→100% B; (8.5~11.0) min, 100% B; (11.0~11.5) min, 100%→50% B; (11.4~14.5) min, 50% B. Time-of-flight MS detection was performed with a Xevo G2-S MS system (Waters Corp., Manchester, UK). The data acquisition range was from 50–1500 Da. The source temperature was set at 100 °C, and the desolvation temperature was set at 450 °C, with desolvation gas flow set at 900 L/h. The lock mass compound used was leucine enkephaline at a concentration 200 pg/μL. The capillary voltage was set at 2.5 KV. The cone voltage was set at 40 V. The collision energy was set as 6 eV for low-energy scan, and 50–65 eV ramp for high-energy scan. The instrument was controlled by Masslynx 4.1 software (Waters Corp., Manchester, UK).

Preparative HPLC separation was performed using a Waters 600E-2487 instrument, using an YMC-Pack ODS-A column (250 mm × 20 mm, 5 μm). The mobile phase was a 4:6 mixture of water and acetonitrile (V/V) for compounds **9** and **10**, or a 6:4 mixture of water and acetonitrile (V/V) for compound **11**, in either case run with a flow rate of 6 mL/min.

For chemical structure characterization, ^{1}H NMR (400 MHz), ^{13}C NMR (100 MHz), and 2D-NMR spectra were recorded with a Bruker DRX 400 spectrometer for 11-hydroxy ferruginol (**6**), ^{1}H NMR (500 MHz), ^{13}C NMR (125 MHz), and 2D-NMR spectra were recorded with a Bruker INOVA-500 spectrometer for 11,20-dihydroxy ferruginol (**9**) and 10-hydroxymethyltetrahydromiltirone (**10**), ^{1}H NMR (600 MHz), ^{13}C NMR (150 MHz), and 2D-NMR spectra were recorded with a Bruker AVIIIHD-600 spectrometer for 20-dihydroxy sugiol (**11**). TMS was used as internal standard. The observed chemical shift values were measured in ppm.

Results

Identification of candidate CYPs

Our previous study indicated that the ferruginol synthase, CYP76AH1, is the first CYP responsible for the generation of oxygenated diterpenoids precursors in tanshinone biosynthesis. We also carried out transcriptomic analysis of the elicitation process in Danshen hairy roots culture and found 125 CYPs expressed therein (Gao *et al.*, 2014). To identify other CYPs involved in tanshinone biosynthesis, here we carried out further co-expression analysis of this transcriptome dataset (Accession No. SRX224100). It was found that the expression of isotig10614 and isotig05577 was highly correlated with that of *CYP76AH1* (Fig. S1). We cloned the corresponding full-length cDNA for these two isotigs, and identified these as *CYP76AH3* (81% sequence similarity to *CYP76AH1*) and *CYP76AK1* (46% sequence similarity to *CYP76AH1*), which represented promising candidates for further functional analysis.

Biochemical characterization of CYP76AH3 & CYP76AK1

Both CYPs were cloned and expressed in the yeast strain WAT11, which overexpresses the plant CYP reductase ATR1 from *A. thaliana* (Urban *et al.*, 1997). Microsomal preparations from the resulting recombinant yeast were used for *in vitro* activity assays with **5** as the substrate. LC-MS analysis of the assay mixtures revealed that CYP76AH3 converted **5** into three compounds, namely, **6**, **7** and **8**, with retention times of 4.75 min, 1.72 min and 1.63 min, respectively (Fig. 2, a–c). Compound **6** had an *m/z* of 301.2188 and it was determined to be 11-hydroxyferruginol based on structural analysis by NMR (Fig. S2). The retention times and mass spectra for compounds **7** and **8** matched those of authentic standards for sugiol and 11-hydroxy sugiol, respectively. Moreover, when microsomal preparations from the yeast cells expressing CYP76AH3 were assayed with **6** or **7** as the substrate, **8** was produced (Fig. S3 and Fig. S4). These results indicated that, at least under *in vitro* conditions, CYP76AH3 functioned as a promiscuous enzyme that not only catalyzes hydroxylation at C-11, but also sequential oxygenation/oxidation reactions at C-7 to form a keto group.

We then assayed microsomes from the yeast cells co-expressing *CYP76AK1* and *CYP76AH3* with **5** as the substrate. LC-MS analysis revealed the presence of three new compounds, namely, **9**, **10** and **11**, with retention times and *m/z* values of 3.31 min and 317.2162, 1.70 min and 315.1954, and 1.22 min and 331.1949, respectively (Fig. 2, c–e). Compound **9** was the major product, and it was determined to be 11,20-dihydroxy ferruginol based on structural analysis by NMR (Fig. S5). Compound **10** was found to be 10-hydroxymethyl tetrahydromiltirone, again based on structural analysis by NMR (Fig. S6). Compound **9** was unstable under ambient conditions and underwent spontaneous oxidization to **10**. Compounds **9** and **10** were produced when microsomal preparations from yeast cells expressing *CYP76AK1* were assayed with **6** as substrate (Fig. S3). We further assayed microsomal preparations from yeast cells expressing *CYP76AK1* alone with **8** as substrate, and demonstrated that it was efficiently converted into **11** (Fig. S7 and S8). However, no products were found when **4**, **5** or **7** were used as substrate. Accordingly, CYP76AK1 can catalyze hydroxylation at the C-20 position of the two differentially oxygenated abietanes **6** and **8**. Thus, while CYP76AK1 exhibits some promiscuity, it seems to only react with phenolic abietane diterpenoids that have hydroxy groups at C-11, as well as C-12.

Physiological function of CYP76AH3 & CYP76AK1

It is well known that tanshinones accumulate predominantly in the root and rhizome of Danshen (Cui *et al.*, 2015). To support physiological roles for CYP76AH3 and CYP76AK1 in tanshinone biosynthesis, we examined the organ specific expression of *CYP76AH3* and *CYP76AK1* by real-time PCR. It was found that the expression of both genes was more abundant in the root than aerial tissues (Fig. 3a), consistent with a role for these two CYPs in the production of tanshinones. In addition, metabolite analysis of Danshen roots by LC-MS revealed the presence of all of the CYP products found here, namely **6** – **11** (Fig. S9), consistent with our in vitro biochemical analyses.

To provide more definitive evidence that CYP76AH3 and CYP76AK1 act in tanshinone biosynthesis, an RNAi approach was used to knock-down expression of the encoding genes

in Danshen hairy roots. Unique fragments from each gene were cloned into a previously described RNAi vector (Cheng *et al.*, 2014), which then expresses self-complementary 'hairpin' RNA fragments that induce silencing, and these constructs were used to transfect Danshen leaf explants to produce recombinant hairy root cultures via *Agrobacterium rhizogene*. RT-PCR analysis indicated that the expression of each targeted gene was efficiently suppressed in the transformed hairy root cultures, while those of known similar CYPs were not notably affected (Fig. 3b and Fig. S10). Targeted metabolite analysis indicated that suppression of *CYP76AK1* led to significantly lower levels of tanshinones **1** – **3** (Fig. 3c), as well as the direct CYP76AK1 products **9** and **11** (Fig. 3d). In addition, levels of the CYP76AK1 substrates, **6** and **8**, were slightly increased in this hairy root culture (Fig. 3d). These results indicate that CYP76AK1 functions as a C-20 hydroxylase for these two intermediates, and the net results suggest a potentially bifurcating pathway in tanshinone biosynthesis. Successful silencing of *CYP76AH3* also was achieved (Fig. 3b), leading to significant reduction in levels of the direct CYP76AH3 products, **6** and **8**, as well as downstream metabolites **9** – **11** (Fig. 3d). This indicates that CYP76AH3 plays a key role in the production of these intermediates. While the levels of tanshinones **1** – **3** were somewhat reduced, this was not statistically significant (Fig. 3c), implying that the reactions catalyzed by CYP76AH3 are not rate limiting in tanshinone biosynthesis.

Homology modeling and docking analysis of CYP76AK1

To gain more insights into the chemo- and regio- selectivity of CYP76AK1, we performed homology modeling and molecular docking with compounds **5** – **8**. The crystal structure of CYP1A2 (code: 2HI4) (Sansen *et al.*, 2007) was selected as the template for homology modeling based on the 44.7% sequence similarity of CYP76AK1 to this human CYP (Fig. S11). As shown in Fig. S12, 88.3% of residues in the homology model are in the most favored region of the Ramachandran plot, with only four outliers in the structure, which suggests that this is a reasonable model for the CYP76AK1 protein structure, and can be used for further structural analysis. Docking results suggested that the distances between the C-20 methyl group in compound **5** and **7** and the catalytic heme iron were 10.8 Å and 9.7 Å, respectively, which are longer than those in the cases of compound **6** and **8** (8.1 Å and 7.0 Å) (Fig. 4). These data are in line with the fact that CYP76AK1 had no activity with **5** and **7**, and to some extent, that the hydroxylation activity with **8** was higher than that with **6**.

Heterologous production of oxygenated tanshinones intermediates in yeast

To further confirm their functions and demonstrate the usefulness of CYP76AH3 and CYP76AK1, these were incorporated into a previously described ferruginol producing yeast strain, YJ35 (Guo *et al.*, 2013). This strain harbors modules that express a GGPP synthase (BTS1) and farnesyl diphosphate synthase (ERG20) fusion, a SmCPS1 and SmKSL1 fusion, a truncated hydroxy-3-methylglutaryl coenzyme A reductase (tHMG1), and the ferruginol synthase CYP76AH1, as well as the Danshen CYP reductase (SmCPR1) (Zhou *et al.*, 2012; Guo *et al.*, 2013). We first incorporated a *CYP76AH3* expression module under the control of the *GAL10* promoter into YJ35 to produce a new strain, YJ51 (Fig. 5a). This YJ51 strain was grown in YNB medium, with glucose as the carbon source, to logarithmic phase, then induced by transferring the cells into medium containing 2% galactose as the carbon source

instead. After 72 h, the fermentation broth was extracted with n-hexane. LC-MS analysis of the extracts showed the presence of three diterpenoids, namely, 57.1% (percentage of total diterpenoid peak area) of **6**, 40.6% of **8** and 2.4% of **7** (Fig. 5a). Indeed, it was this strain that provided sufficient amount of **6** for detailed structural characterization by NMR (Fig. S2).

We further added *CYP76AK1* into the *CYP76AH3* expression plasmid, and transformed this into YJ35 to generate the yeast strain YJ61 (Fig. 5b). The resulting strain was cultivated, and extracts prepared, as described above for the YJ51 strain. LC-MS analysis indicated that YJ61 produced 78.4% of **9**, 18.2% of **10**, 1.6% of **11,** 1.4% of **7**, and 0.4% of **6** (Fig. 5b), which indicated that most of the intermediates were efficiently converted to the more elaborated compounds **9** and **10**. Again, it was this YJ61 strain that provided sufficient amounts of **9** and **10** for structural characterization by NMR.

The use of the *GAL1p* and *GAL10p* promoters for expressing *CYP76AH3* and *CYP76AK1* required the use of galactose as the carbon source, necessitating a two-stage fermentation process. To avoid this, we replaced these *GAL* promoters with the constitutive promoters *TEF1p* and *PGK1p* (Zhou *et al.*, 2011). This new expression plasmid was transformed into YJ35 to generate the yeast strain YJ62 (Fig. 5c). When YJ62 was cultivated for 72 h in medium containing glucose as the carbon source, oxygenated diterpenoids were produced with a distribution profile quite similar to that of YJ61, as the peak areas for **9** and **10** were 92.8% of the total. Though total diterpenoid accumulation was lower than with YJ61, the YJ62 strain provides a more straightforward platform for the production of these diterpenoid metabolites, which should facilitate future studies of tanshinone biosynthesis, as well as the biological activity of these diterpenoid metabolites.

Discussion

CYPs play key roles in producing the tremendous chemical diversity of terpenoids products. These heme-containing enzymes typically insert an oxygen atom into C-H bond, generating a hydroxyl group that enable further transformations, such as oxidation, acylation, methylation and glycosylation. In addition, CYPs can catalyze more unusual transformations as well (Ashour *et al.*, 2010). However, functional characterization of eukaryotic CYPs remains challenging. This is particularly true in plants, where the CYP superfamily represents approximately 1% of all protein encoding genes (Renault *et al.*, 2014). Moreover, terpenoid biosynthetic pathways routinely require multiple CYP-mediated biochemical transformations, further complicating the assignment of their functional roles (Pateraki *et al.*, 2015). For example, the CYPs implicated in catalyzing different steps of taxol biosynthesis share >70% amino acid sequence identity, yet this metabolic pathway remains incompletely elucidated (Kaspera & Croteau, 2006). Recently, thanks to advances in DNA sequencing technology, co-expression analysis has been shown to be useful for identifying pathway-associated CYPs (Ehlting *et al.*, 2008).

As extensively aromatized abietane-type *ortho*-quinone and furan ring containing *nor*-diterpenoids, the tanshinones are formed from the olefinic precursor miltiradiene (**4**) via a series of oxidative transformations. In previous work, we demonstrated that CYP76AH1

produces ferruginol (**5**) (Guo *et al.*, 2013; Zi & Peters, 2013). To identify CYPs responsible for subsequent steps in tanshinone biosynthesis, we carried out co-expression analysis of the transcriptome dataset to find CYPs whose expression profile matched that of *CYP76AH1* and identified two candidates from the CYP76 family, *CYP76AH3* and *CYP76AK1*. We constructed yeast strains that expressed these CYPs, both separately and together. Using **5** as the substrate, microsomes from the *CYP76AH3* expressing yeast produced three new products, compounds **6** – **8**. When using microsomes that contain both CYPs, three additional products were observed, compounds **9** – **11**. While the structures for **7** and **8** were readily established by comparison with those of authentic standards, the identities of the other four compounds remained elusive. To acquire sufficient amounts of these compounds for structural elucidation, we employed a synthetic biology approach to construct recombinant yeast for heterologous production of **6**, **9** and **10**, while **11** was produced via *in vitro* conversion of **8** at a preparative scale. Critically, RNAi knock-down of *CYP76AH3* and *CYP76AK1* expression in Danshen hairy root cultures afforded results in agreement with the functional assignment based on the biochemical information (*vide ante*). Taken together, these results highlight the utility of this approach towards characterization of CYPs involved in plant terpenoid biosynthesis.

Both CYP76AH3 and CYP76AK1 exhibit promiscuity. CYP76AH3 can take **5** and carry out hydroxylation at C-11 to form **6**, or at C-7, with further oxidation to form the keto group of **7**. In either case, these initial products can be further transformed, via the alternative reaction, to produce **8**. It should be noted that other CYP76 family members have also been shown to exhibit promiscuous activity in diterpenoids biosynthesis (Swaminathan *et al.*, 2009; Wang *et al.*, 2012; Wu *et al.*, 2013), but CYP76AH3 is unique because it shows promiscuity in substrate selectivity as well as catalytic activity. The complex mixture of products observed here suggests that CYP76AH3 may play a role in producing the wide range of tanshinones and structurally related compounds found in Danshen (Dong *et al.*, 2011). In addition, the multifunctional nature of CYP76AH3 indicates that this also might be useful as a biocatalyst to produce new diterpenoids – e.g., via metabolic engineering in yeast. By contrast, CYP76AK1 exhibits substrate promiscuity, carrying out hydroxylation at C-20 of either **6** or **8**, to produce **9** or **11**, respectively. Notably, the promiscuity exhibited by CYP76AH3 and CYP76AK1 leads to bifurcation of tanshinone biosynthesis. In particular, the CYP76AH3 products **6** and **8** can be observed in Danshen, serve as substrates for CYP76AK1, and both accumulate upon knocking down *CYP76AK1* expression, which further represses the accumulation of tanshinones. Because of CYP promiscuity, divergent pathways become possible in plants, resulting in additional difficulties for pathway delineation. Such metabolic networks may be advantageous to bypass damages and mutations that may otherwise lead to the breakdown of the biosynthetic process. Perhaps more intriguingly, this also may provide arrays of similar natural products that might interfere with the ability of simple mutations in their molecular targets to escape inhibition.

It is conceivable that both **9** and **11** are precursors to tanshinones, as hydroxylation of C-20 is a necessary step in oxidative removal of this methyl group, as well as the potentially associated aromatization of the B-ring. Indeed, the C-7 keto group in **11** represents further oxidation towards B-ring aromatization. However, the relevance of CYP76AH3 for this

transformation is not entirely clear, as knocking down *CYP76AH3* expression has only limited effect on the production of **7**. Consistent with this, C-7 keto containing diterpenoids are accumulated at low levels in the engineered yeast strains, indicating that CYP76AH3 predominantly produces **6**, and has relatively low catalytic activity on **6** and **7**. In addition, knocking down *CYP76AH3* expression only slightly reduces the accumulation of tanshinones, which may reflect a non-rate limiting role for CYP76AH3, and/or some redundancy. Given the presence of multiple CYP76 family members in Danshen (Chen *et al.*, 2014), it seems likely that these CYPs may be responsible for C-7 oxidation and/or provide such redundant activity. Regardless, our results indicate that CYP76AK1 plays a key role in tanshinone production, suggesting that overexpression of this might improve yields, which is particularly important as the contents of tanshinones in Danshen are low and vary depending on the place of origin, the harvest season and the traditional processing methods (Hu *et al.*, 2005; Wu *et al.*, 2009).

In summary, we have functionally identified two CYPs involved in production of tanshiones, and whose promiscuity indicates bifurcation in this biosynthetic process, suggesting it comprises a complex metabolic network. Altogether, we have now identified three CYPs, including the previous reported CYP76AH1 (Guo *et al.*, 2013), which insert up to four atoms of oxygen into the abietane hydrocarbon intermediate **4** en route to the tanshinones. This represents substantial advancement towards elucidating tanshinone biosynthesis (Gao *et al.*, 2009; Wang & Wu, 2010), and enriches our understanding of the complex roles of CYPs in the metabolic networks underlying terpenoid production more generally. Moreover, we have demonstrated that the CYPs identified here can be used in a synthetic biology approach towards heterologous production of tanshinones in yeast. Indeed, the resulting diterpenoids not only provide intermediates for further investigation of tanshinone biosynthesis, but also material for investigation of their own biological activity.

Supplementary Material

Refer to Web version on PubMed Central for supplementary material.

Acknowledgments

We thank Prof. Wenhan Lin and Mr. Haiyu Xu for suggestions about experimental protocols. We acknowledge funding by the National Natural Science Foundation of China (81325023, 21325627, 81130070, 81573532, 81202871 and 81403049), the National High Technology Research and Development Program (2012AA02A704 and SS2014AA022201) and the National Institutes of Health (GM109773 to R.J.P.).

References

Altschul SF, Madden TL, Schäffer AA, Zhang J, Zhang Z, Miller W, Lipman DJ. Gapped BLAST and PSI-BLAST: a new generation of protein database search programs. Nucleic Acids Research. 1997; 25(17):3389–3402. [PubMed: 9254694]

Ashour, M.; Wink, M.; Gershenzon, J. Biochemistry of terpenoids: monoterpenes, sesquiterpenes and diterpenes. In: Wink, M., editor. Annual Plant Reviews Volume 40: Biochemistry of Plant Secondary Metabolism. Oxford, UK: Wiley-Blackwell; 2010. p. 258-303.

Bak S, Beisson F, Bishop G, Hamberger B, Höfer R, Paquette S, Werck-Reichhart D. Cytochromes P450. The Arabidopsis Book/American Society of Plant Biologists. 2011; 9:e0144. [PubMed: 22303269]

Chen H, Wu B, Nelson DR, Wu K, Liu C. Computational identification and systematic classification of novel cytochrome P450 genes in *Salvia miltiorrhiza*. PloS One. 2014; 9(12):28.

Cheng Q, He Y, Li G, Liu Y, Gao W, Huang L. Effects of combined elicitors on tanshinone metabolic profiling and *SmCPS* expression in *Salvia miltiorrhiza* hairy root cultures. Molecules. 2013; 18(7): 7473–7485. [PubMed: 23807574]

Cheng Q, Su P, Hu Y, He Y, Gao W, Huang L. RNA interference-mediated repression of *SmCPS* (*copalyldiphosphate synthase*) expression in hairy roots of *Salvia miltiorrhiza* causes a decrease of tanshinones and sheds light on the functional role of SmCPS. Biotechnology Letters. 2014; 36(2): 363–369. [PubMed: 24078134]

Cui G, Duan L, Jin B, Qian J, Xue Z, Shen G, Snyder JH, Song J, Chen S, Huang L, et al. Functional divergence of diterpene syntheses in the medicinal plant *Salvia miltiorrhiza* Bunge. Plant Physiology. 2015

Dai Z, Liu Y, Huang L, Zhang X. Production of miltiradiene by metabolically engineered *Saccharomyces cerevisiae*. Biotechnology and Bioengineering. 2012; 109(11):2845–2853. [PubMed: 22566191]

Daniel Gietz R, Woods RA. Transformation of yeast by lithium acetate/single-stranded carrier DNA/ polyethylene glycol method. Methods in Enzymology. 2002; 350:87–96. [PubMed: 12073338]

Dong Y, Morris-Natschke SL, Lee K-H. Biosynthesis, total syntheses, and antitumor activity of tanshinones and their analogs as potential therapeutic agents. Natural Product Reports. 2011; 28(3):529–542. [PubMed: 21225077]

Ehlting J, Sauveplane V, Olry A, Ginglinger J-F, Provart N, Werck-Reichhart D. An extensive (co-)expression analysis tool for the cytochrome P450 superfamily in *Arabidopsis thaliana*. BMC Plant Biology. 2008; 8(47)

Gao W, Hillwig ML, Huang L, Cui G, Wang X, Kong J, Yang B, Peters RJ. A functional genomics approach to tanshinone biosynthesis provides stereochemical insights. Organic Letters. 2009; 11(22):5170–5173. [PubMed: 19905026]

Gao W, Sun H-X, Xiao H, Cui G, Hillwig M, Jackson A, Wang X, Shen Y, Zhao N, Zhang L, et al. Combining metabolomics and transcriptomics to characterize tanshinone biosynthesis in *Salvia miltiorrhiza*. BMC Genomics. 2014; 15(1):73. [PubMed: 24467826]

Gershenzon J, Dudareva N. The function of terpene natural products in the natural world. Nature Chemical Biology. 2007; 3(7):408–414. [PubMed: 17576428]

Guo J, Zhou YJ, Hillwig ML, Shen Y, Yang L, Wang Y, Zhang X, Liu W, Peters RJ, Chen X, et al. CYP76AH1 catalyzes turnover of miltiradiene in tanshinones biosynthesis and enables heterologous production of ferruginol in yeasts. Proceedings of the National Academy of Sciences. 2013; 110(29):12108–12113.

Hamberger B, Bak S. Plant P450s as versatile drivers for evolution of species-specific chemical diversity. Philosophical Transactions of the Royal Society B. Biological Sciences. 2013; 368(1612)

Hu P, Luo GA, Zhao ZZ, Jiang ZH. Quantitative determination of four diterpenoids in Radix *Salvia Miltiorrhizae* using LC-MS-MS. Chemical and Pharmaceutical Bulletin. 2005; 53(6):705–709. [PubMed: 15930789]

Kai G, Xu H, Zhou C, Liao P, Xiao J, Luo X, You L, Zhang L. Metabolic engineering tanshinone biosynthetic pathway in *Salvia miltiorrhiza* hairy root cultures. Metabolic Engineering. 2011; 13(3):319–327. [PubMed: 21335099]

Kaspera R, Croteau R. Cytochrome P450 oxygenases of Taxol biosynthesis. Phytochemistry Reviews. 2006; 5(2):433–444. [PubMed: 20622990]

Kitaoka N, Lu X, Yang B, Peters RJ. The application of synthetic biology to elucidation of plant mono-, sesqui-, and diterpenoid metabolism. Molecular Plant. 2015; 8(1):6–16. [PubMed: 25578268]

Laskowski RA, MacArthur MW, Moss DS, Thornton JM. PROCHECK: a program to check the stereochemical quality of protein structures. Journal of Applied Crystallography. 1993; 26(2):283–291.

Mizutani M, Sato F. Unusual P450 reactions in plant secondary metabolism. Archives of Biochemistry and Biophysics. 2011; 507(1):194–203. [PubMed: 20920462]

Morris GM, Goodsell DS, Halliday RS, Huey R, Hart WE, Belew RK, Olson AJ. Automated docking using a Lamarckian genetic algorithm and an empirical binding free energy function. Journal of Computational Chemistry. 1998; 19(14):1639–1662.

Pateraki I, Heskes AM, Hamberger B. Cytochromes P450 for terpene functionalisation and metabolic engineering. Advances in Biochemical Engineering Biotechnology. 2015; 148:107–139.

Pompon D, Louerat B, Bronine A, Urban P. Yeast expression of animal and plant P450s in optimized redox environments. Methods in Enzymology. 1996; 272:51–64. [PubMed: 8791762]

Renault H, Bassard JE, Hamberger B, Werck-Reichhart D. Cytochrome P450-mediated metabolic engineering: current progress and future challenges. Current Opinion in Plant Biology. 2014; 19(0):27–34. [PubMed: 24709279]

Ro DK, Arimura GI, Lau SYW, Piers E, Bohlmann J. Loblolly pine abietadienol/abietadienal oxidase PtAO (CYP720B1) is a multifunctional, multisubstrate cytochrome P450 monooxygenase. Proceedings of the National Academy of Sciences. 2005; 102(22):8060–8065.

Robertson AL, Holmes GR, Bojarczuk AN, Burgon J, Loynes CA, Chimen M, Sawtell AK, Hamza B, Willson J, Walmsley SR, et al. A zebrafish compound screen reveals modulation of neutrophil reverse migration as an anti-inflammatory mechanism. Science Translational Medicine. 2014; 6(225):225–229.

Sansen S, Yano JK, Reynald RL, Schoch GA, Griffin KJ, Stout CD, Johnson EF. Adaptations for the oxidation of polycyclic aromatic hydrocarbons exhibited by the structure of human P450 1A2. Journal of Biological Chemistry. 2007; 282(19):14348–14355. [PubMed: 17311915]

Seki H, Sawai S, Ohyama K, Mizutani M, Ohnishi T, Sudo H, Fukushima EO, Akashi T, Aoki T, Saito K. Triterpene functional genomics in Licorice for identification of CYP72A154 involved in the biosynthesis of glycyrrhizin. The Plant Cell. 2011; 23(11):4112–4123. [PubMed: 22128119]

Swaminathan S, Morrone D, Wang Q, Fulton DB, Peters RJ. CYP76M7 is an*ent*-cassadiene C11α-hydroxylase defining a second multifunctional diterpenoid biosynthetic gene cluster in rice. The Plant Cell. 2009; 21:3315–3325. [PubMed: 19825834]

Urban P, Mignotte C, Kazmaier M, Delorme F, Pompon D. Cloning, yeast expression, and characterization of the coupling of two distantly related *Arabidopsis thaliana* NADPH-cytochrome P450 reductases with P450 CYP73A5. Journal of Biological Chemistry. 1997; 272(31):19176–19186. [PubMed: 9235908]

Wang JW, Wu JY. Tanshinone biosynthesis in *Salvia miltiorrhiza* and production in plant tissue cultures. Applied Microbiology and Biotechnology. 2010; 88(2):437–449. [PubMed: 20694462]

Wang Q, Hillwig ML, Okada K, Yamazaki K, Wu Y, Swaminathan S, Yamane H, Peters RJ. Characterization of CYP76M5-8 indicates metabolic plasticity within a plant biosynthetic gene cluster. Journal of Biological Chemistry. 2012; 287(9):6159–6168. [PubMed: 22215681]

Weigel D, Glazebrook J. Transformation of agrobacterium using the freeze-thaw method. Cold Spring Harbor Protocols. 2005; 2006(7):1031–1036.

Wu K, Zhang Q, Liu Q, Tang F, Long Y, Yao S. Ionic liquid surfactant-mediated ultrasonic-assisted extraction coupled to HPLC: application to analysis of tanshinones in *Salvia miltiorrhiza* bunge. Journal of Separation Science. 2009; 32(23–24):4220–4226. [PubMed: 19937963]

Wu Y, Wang Q, Hillwig ML, Peters RJ. Picking sides: Distinct roles for CYP76M6 and-8 in rice oryzalexin biosynthesis. Biochemical Journal. 2013; 454(2):209–216. [PubMed: 23795884]

Zhou L, Zuo Z, Chow MSS. Danshen: An overview of its chemistry, pharmacology, pharmacokinetics, and clinical use. The Journal of Clinical Pharmacology. 2005; 45(12):345–1359.

Zhou YJ, Gao W, Rong Q, Jin G, Chu H, Liu W, Yang W, Zhu Z, Li G, Zhu G, et al. Modular pathway engineering of diterpenoid synthases and the Mevalonic Acid Pathway for miltiradiene production. Journal of the American Chemical Society. 2012; 134(6):3234–3241. [PubMed: 22280121]

Zhou YJ, Yang F, Zhang S, Tan H, Zhao ZK. Efficient gene disruption in *Saccharomyces cerevisiae* using marker cassettes with long homologous arms prepared by the restriction-free cloning strategy. World Journal of Microbiology and Biotechnology. 2011; 27(12):2999–3003.

Zi J, Peters RJ. Characterization of CYP76AH4 clarifies phenolic diterpenoid biosynthesis in the Lamiaceae. Organic & Biomolecular Chemistry. 2013; 11(44):7650–7652. [PubMed: 24108414]

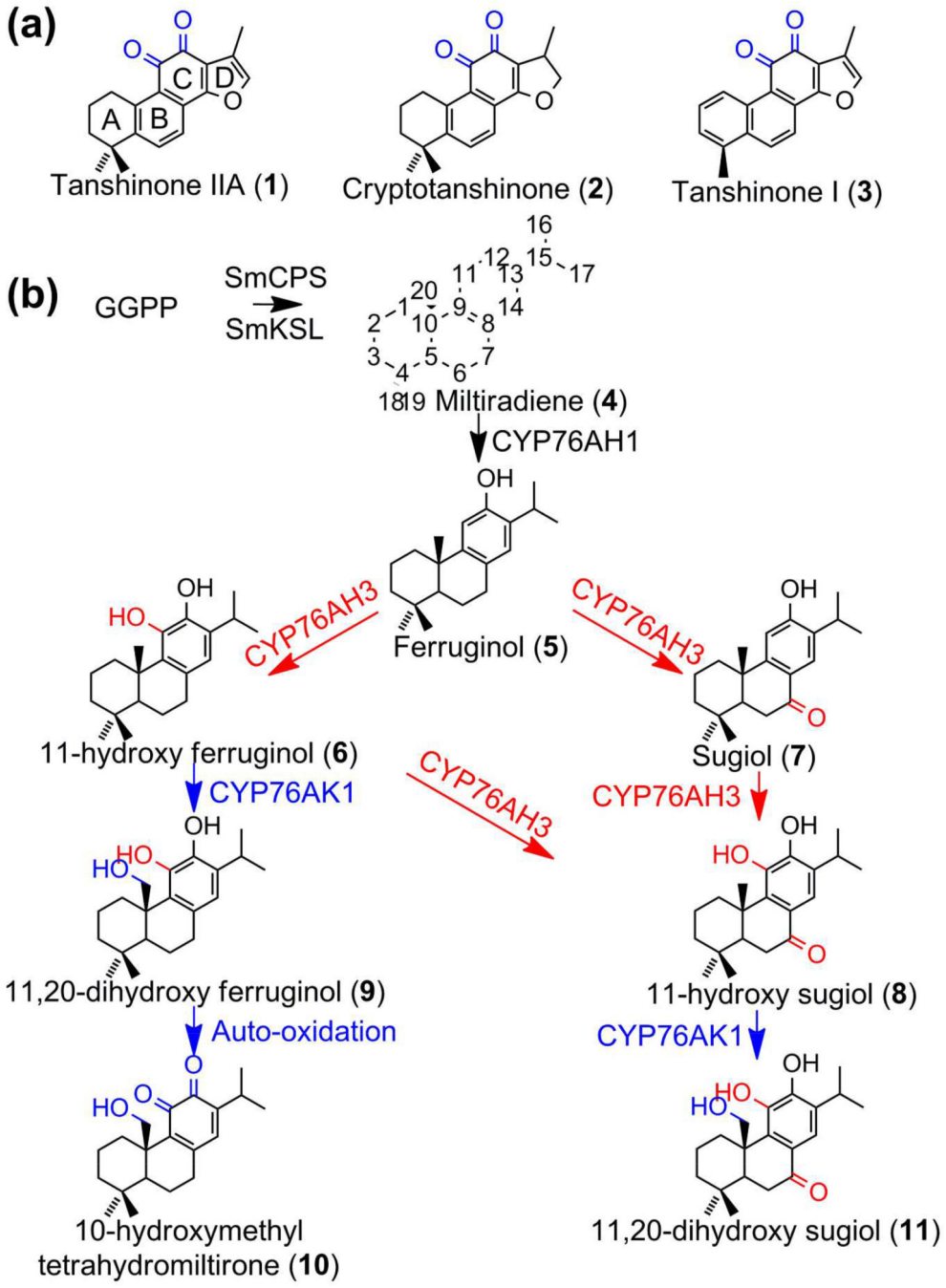

Fig. 1.

Tanshinones and partial biosynthetic pathway in *S. miltiorrhiza*. (a) Representative tanshinones found in *S. miltiorrhiza*. (b) Proposed partial biosynthetic pathway of tanshinones. The red arrow indicates the oxidation reaction catalyzed by the CYP76AH3 enzyme. The blue arrow indicates the oxidation reaction catalyzed by the CYP76AK1 enzyme.

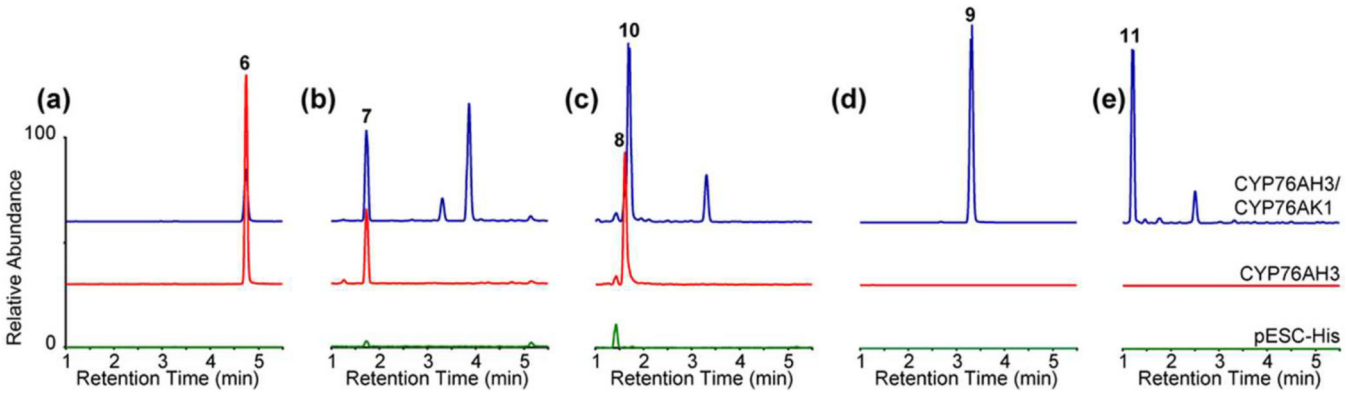

Fig. 2.

LC-MS analysis results of reaction mixtures of **5** catalyzed by yeast microsomes containing CYPs from *S. miltiorrhiza*. (a) The extracted ion current (EIC) chromatogram of 11-hydroxy ferruginol (**6**). (b) The EIC of sugiol (**7**). (c) The EIC of 11-hydroxy sugiol (**8**) and 10-hydroxymethyl tetrahydromiltirone (**10**). (d) The EICs of 11,20-dihydroxy ferruginol (**9**). (e) The EIC of 11,20-dihydroxy sugiol (**11**). The resulting daughter ion mass spectra are shown in Fig. S2, S5, S6, and S8 for compound **6**, **9**, **10**, and **11**, respectively. The green, blue and red lines represent the yeast harboring the plasmid pESC-His, pESC-His::*CYP76AK1* and pESC-His::*CYP76AH3/CYP76AK1*, respectively.

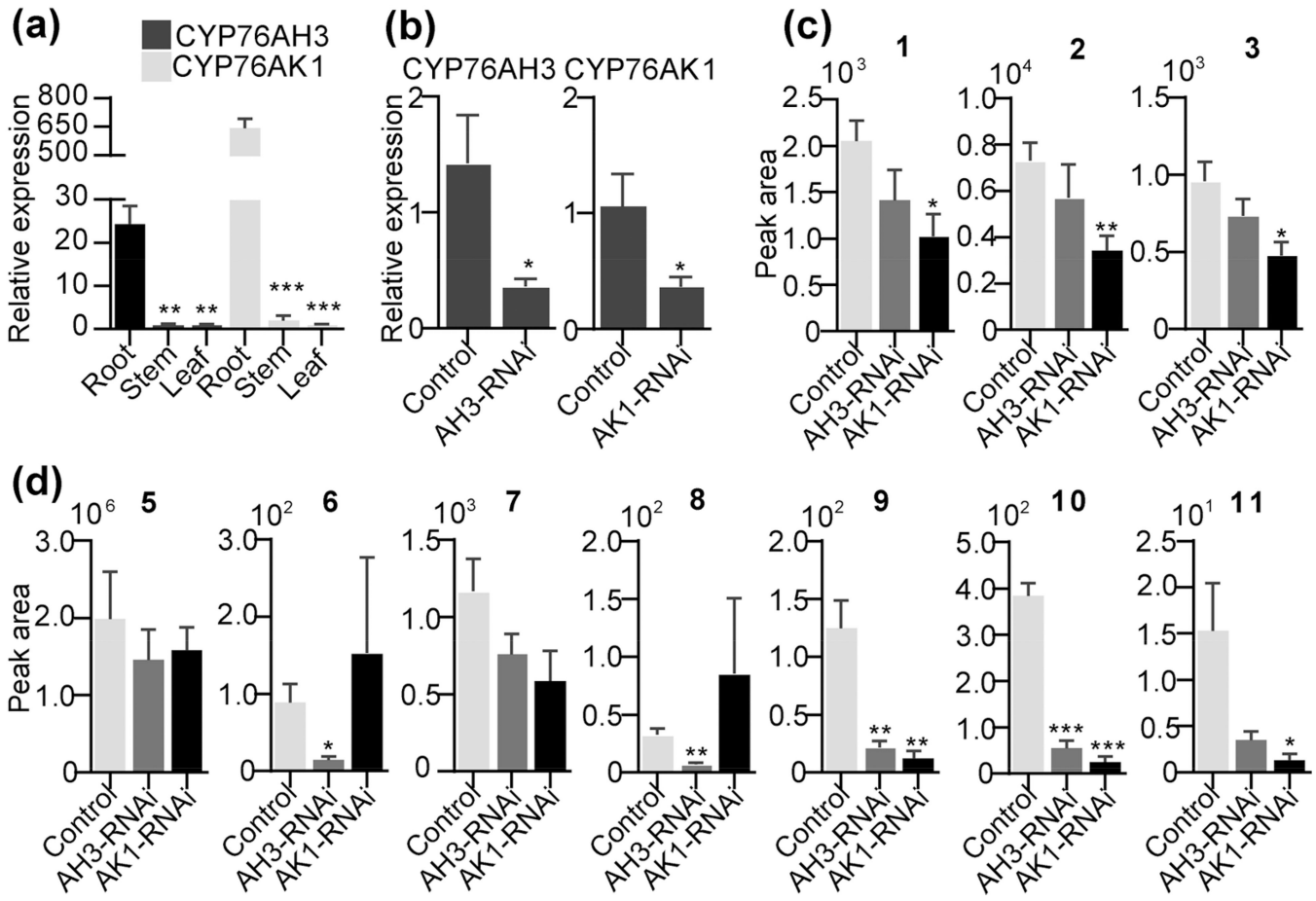

Fig. 3.

The relationship between the expression levels of *CYP76AH3* and *CYP76AK1* and the contents of different terpenoids products. (a) Expression levels of *CYP76AH3* and *CYP76AK1* in root, stem and leaf of in *S. miltiorrhiza*. (b) Expression levels of *CYP76AH3* and *CYP76AK1* in RNAi down-regulated in *S. miltiorrhiza* hairy roots. (c) Contents of tanshinones **1**, **2** and **3** in RNAi down-regulated in *S. miltiorrhiza* hairy roots. (d) Contents of oxygenated terpenoids intermediates **5 – 11** in RNAi down-regulated in *S. miltiorrhiza* hairy roots. Expression levels were normalized using β-actin as an internal standard. The error bars represent the standard error of means from three independent replications for tissue expression analysis and from 5 to 6 lines for RNAi down-regulated hairy roots. * $P < 0.05$, ** $P < 0.01$ and *** $P < 0.001$ were determined by an unpaired *t* test using GraphPad Prism 6.

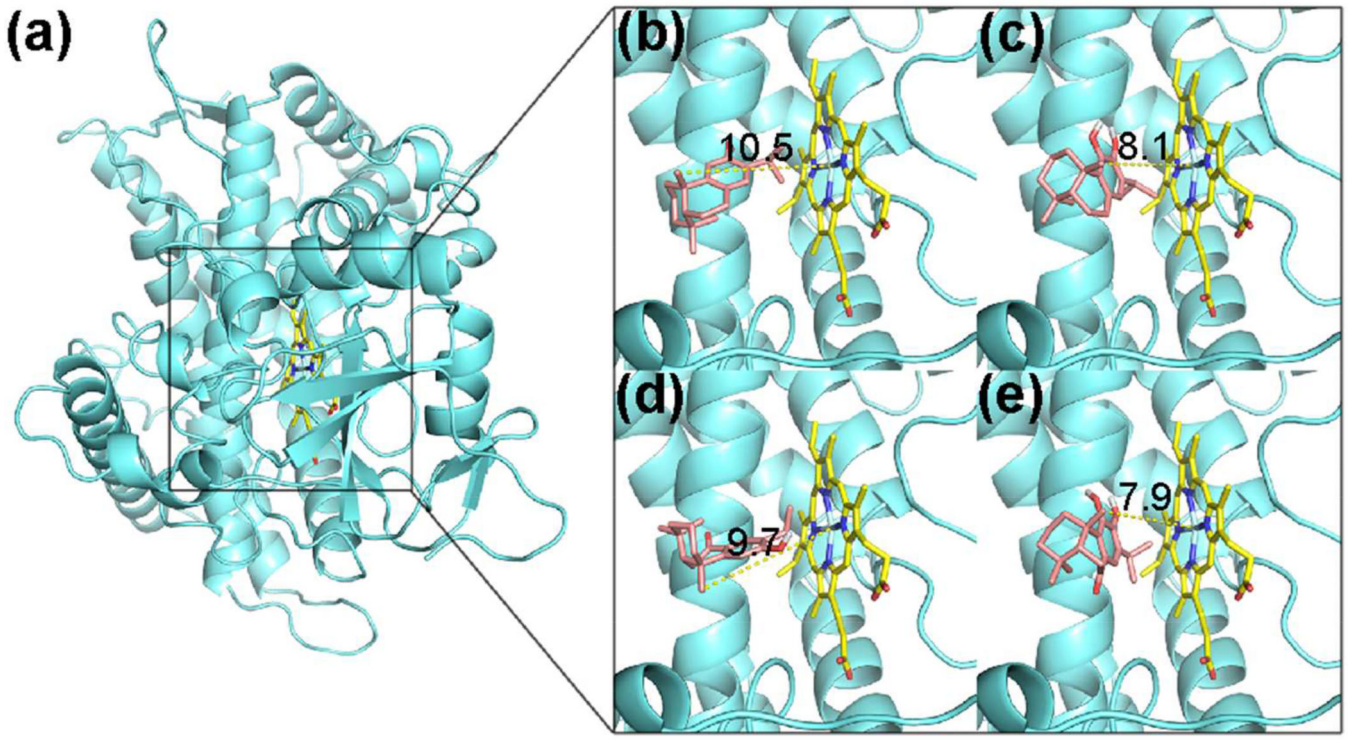

Fig. 4.

Homology modeling and docking analysis of CYP76AK1 from *S. miltiorrhiza*. (a) Homology modeling of CYP76AK1. Docking poses of compound **5** (b), **6** (c), **7** (d), **8** (e). Compound structure is depicted as stick with carbons colored pink and oxygens red. Heme is depicted as stick with carbons colored yellow and iron blue. Distance between C20 and heme iron is indicated by dashed line with the length indicated in Å.

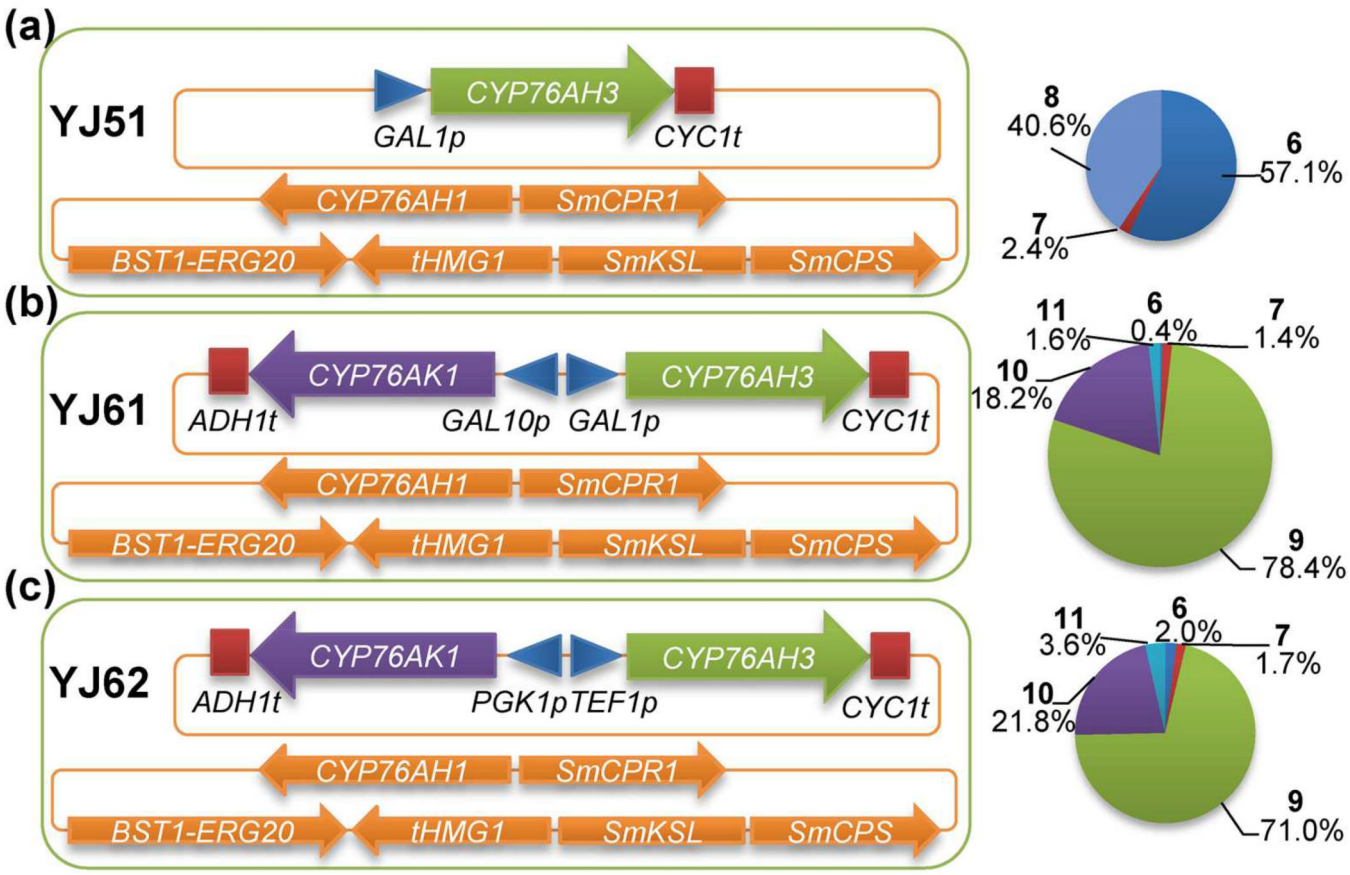

Fig. 5.

Engineered yeasts for the production of oxygenated terpenoids intermediates. YJ35 was constructed previously (Guo *et al.*, 2013). The YJ51 (a) and YJ61 (b) were constructed by transforming pESC-His::*CYP76AH3* and pESC-His::*CYP76AH3*/*CYP76AK1* into YJ35, respectively. YJ62 (c) was constructed by replacing the *GAL1* and *GAL10* promoter in pESC-His::*CYP76AH3*/*CYP76AK1* with the constitutive promoter *TEF1* and *PGK1* and transforming into YJ35. The pie chart and its area represent the percentages of ferruginol derivatives (compounds **6**, **7**, **8**, **9**, **10**, and **11**) and the accumulation of diterpenoids produced in the YJ51 (a), YJ61 (b) and YJ62 (c) after 72 h of shake-flask fermentation at 250 rpm in YNB with galactose for YJ51 and YJ61, and YNB with glucose for YJ62. The data represent the mean value of three independent replications.